

Contents

1	Theoretical background	1
1.1	Atoms and light	1
1.2	Helium	5
1.3	Interacting atoms	7
1.4	Bose-Einstein condensation	9

Chapter 1

Theoretical background

“No one’s mouth is big enough to utter the whole thing.”

- Alan Watts

A cold atom experimentalist draws on a panoply of tools (both conceptual and instrumental) which are all intricate and absorbing in their own right. This chapter presents the essential ideas needed to give form and context to the content of the major works reported in this thesis. We will glance at the Hydrogen atom to establish a language with which to elucidate the deceptively simple structure of Helium. We must be equipped with some study of the coupling between electromagnetic fields and light, given the ubiquitous use of laser sources and magnetic trapping in this dissertation, and the focus¹ on laser spectroscopy.

Of course, the fun doesn’t end when the lights turn off: Even in the dark, helium exhibits explosive two-body interactions, which both pave the road towards absolute zero while imposing limits on the size and lifetime of atomic condensates. Finally, we will review the basic features of the emergence of macroscopic coherence in the form of a Bose-Einstein condensate.

1.1 Atoms and light

The discussion in this section is a short tour of atomic physics. Many high-quality textbooks, including [21, 13], go into much greater detail than is required for this thesis. In this section, only the essential points are presented, omitting lengthy calculations, with references provided for the complete working. Our picture of atoms, their structure, and the interaction with electromagnetic fields, will be made in terms of their modern description in the language of quantum mechanics.

Quantum mechanics is the study of systems whose state at a any time t is completely specified by wavefunction $|\psi(t)\rangle$ and whose dynamics are determined by the time-dependent Schrödinger equation,

$$i\hbar \frac{\partial}{\partial t} |\psi(t)\rangle = \hat{H} |\psi(t)\rangle. \quad (1.1)$$

The wavefunction $|\psi\rangle$ is represented by a *state vector* that is an element of the complex Hilbert space \mathcal{H} . The *Born rule* postulates that the probability of a quantum system being observed in the state $|\psi\rangle$ given that it is known to be in the state $|\phi\rangle$ is given by squared inner product $|\langle\psi|\phi\rangle|^2$. States are orthogonal if the inner product is zero, but the system may evolve naturally from $|\phi\rangle$ to have a nonzero projection onto $|\psi\rangle$ under the action of \hat{H} . The Hamiltonian \hat{H} is a linear operator with the Hermitian property $\hat{H}^\dagger = \hat{H}$, where the

¹The *focus* of a lens or mirror is the point of maximum concentration of light that is refracted or reflected from a distant or uniform source. Originally, the term referred to the fireplace at the centre of traditional single-room dwellings; still the brightest point of light, but also the source itself.

dagger denotes the conjugate transpose operation². The Hermitian property guarantees \hat{H} is *normal*, $[\hat{H}^\dagger, \hat{H}] = 0$ and therefore the time-independent Schrödinger equation

$$\hat{H}|\psi\rangle = E|\psi\rangle \quad (1.2)$$

specifies the eigenvectors $|e_n\rangle$ of \hat{H} which provide a complete orthonormal basis for \mathcal{H} . This allows any (pure) quantum state to be written in the form $|\psi\rangle = \sum_n a_n |e_n\rangle$. An interpretation of this fact in the light of the Born rule is that the energy eigenstates $|e_i\rangle$ correspond to distinguishable and mutually exclusive states of a system, which can be discriminated if their energy eigenvalues E_i are different. In the cases where eigenvalues coincide, there exists at least one other observable that distinguishes the degenerate energy eigenstates.

The energy eigenbasis for a single charged particle bound in a central potential³ have the form,

$$\psi_{nlm}(r, \theta, \phi) = \sqrt{\left(\frac{2}{na_0^*}\right)^3 \frac{(n-l-1)!}{2n(n+l)!}} e^{-\rho/2} \rho^l L_{n-l-1}^{2l+1}(\rho) Y_l^m(\theta, \phi) \quad (1.3)$$

when written in spherical coordinates (r, θ, ϕ) , where $\rho = 2r/na_0^*$ and $a_0^* = \frac{4\pi\epsilon_0\hbar^2}{\mu e^2}$ is the reduced Bohr radius. The radial Laguerre polynomials $L_{n-l-1}^{2l+1}(r)$ and the spherical harmonics $Y_{l,m}(\theta, \phi)$ are labeled by the angular momentum l , the magnetic quantum number m , and the energy is fixed by the principal quantum number n as $E_n = -hcR_\infty/n^2$. The bound-state energy E_n is negative - one must do work to ionize the atom and produce the free ion-electron pair whose energy is defined to be zero. The quantum numbers l and m distinguish states that are otherwise degenerate in n , and serve to lift the degeneracy via the Zeeman shift as I discuss in a later section. Here, $h = 2\pi\hbar$ is the Planck constant, ϵ_0 is the electric permittivity of free space, and μ is the Bohr magneton.

Let us consider an atom immersed in an electric field oscillating with frequency $\omega = 2\pi f$ rad Hz, and write the Hamiltonian in the form

$$\hat{H}(t) = \hat{H}_0 + \hat{H}_I(t) \quad (1.4)$$

where the bare atomic Hamiltonian H_0 sets the energy scale of the system, and the monochromatic time-dependent perturbation takes the form $\hat{H}_I(t) = \Lambda \cos(\omega t)$. We will give physical meaning to Λ in a moment. The time-dependent state can be written in terms of the eigenbasis $|\psi_n\rangle$ of \hat{H}_0 ,

$$|\Psi(t)\rangle = \sum_n c_n(t) e^{-i\omega_n t} |\psi_n\rangle, \quad (1.5)$$

where $\omega_n = E_n/\hbar$. Substitution into Eqn 1.1 reduces to the coupled set of differential equations

$$i\hbar\dot{c}_n(t) = \sum_m e^{-i(E_m - E_n)t/\hbar} \langle \psi_m | \hat{H}_I | \psi_n \rangle, \quad (1.6)$$

which can be solved succinctly after making two simplifications. First, let us assume (without loss of generality) that the atom is initially in the state ψ_1 , where $c_1(0) = 1$ and $c_i(0) = 0 \forall i \neq 1$. Then at a time t the probability that the atom is in the state ψ_k is [21, 13]

$$P_k(t) = 4 |\langle \psi_k | \hat{H}_I | \psi_1 \rangle|^2 \frac{\sin^2(\frac{1}{2}(\omega_k - \omega)t)}{(\omega_k - \omega)^2}, \quad (1.7)$$

²Formally, \mathcal{H} is a vector space \mathbb{C}^D of dimension D which is complete with respect to the L^2 norm $\|x\| = \sqrt{\langle x|x \rangle}$ induced by the inner product $\langle x|y \rangle \rightarrow \mathbb{C}$, and $\hat{H} \in \mathcal{B}$, the Banach space of bounded linear operators $\hat{O} : \mathcal{H} \rightarrow \mathcal{H}$. \mathcal{B} is also a vector space with a norm (the trace norm) but not an inner product. The states themselves are defined up to scalar multiplication, and hence are actually rays in \mathcal{H} better thought of as points in projective space; we will simply assume they are normalized as $\langle \psi|\psi \rangle = 1$ for brevity. We will say no more of the tremendous consternations which stem from the Born rule.

³Better known as the hydrogen atom

where $\omega_k = (E_1 - E_k)/\hbar$. An immediate consequence is that the denominator in Eqn, (1.7) suppresses excitation into $|\psi_k\rangle$ unless ω is close to the resonant frequency ω_k . This weak driving permits us to make a further simplification and consider an atom with only *two* states, labeled 1 and 2, with a resonant frequency $\omega_0 = (E_2 - E_1)/\hbar$. Further, the numerator captures the essential feature that the state oscillates between states in response to the driving field. We are now ready to impart a physical meaning to the coupling term: An atom exposed to an oscillating field will respond by oscillating between energy eigenstates, each of which having their own charge distribution through space. This produces an oscillating electric dipole whose interaction with the electric field can be simplified by working in the *dipole approximation*: Assume the electric field has a constant value throughout space, but oscillates in time as $\mathbf{E}(t) = \mathbf{E}_0 \text{Re}(e^{-i\omega t} \hat{\varepsilon})$, where $\hat{\varepsilon}$ is the unit polarization vector, and $\mathbf{r} = r\hat{\mathbf{r}}$. The interaction energy is then given by retaining only the dipole operator $-\mathbf{er}$ from the multipole expansion of the electronic charge distribution⁴. The interaction Hamiltonian can then be written as

$$\hat{H}_I = \mathbf{er} \cdot \mathbf{E}(t), \quad (1.8)$$

and the excitation probability can be written in the more familiar form [21, 13]

$$P_2(t) = \Omega^2 \frac{\sin^2(\frac{1}{2}(\omega_0 - \omega)t)}{(\omega_0 - \omega)^2}, \quad (1.9)$$

in terms of the Rabi frequency

$$\Omega = \frac{\langle \psi_1 | \mathbf{er} \cdot \mathbf{E} | \psi_2 \rangle}{\hbar}, \quad (1.10)$$

which is, in general, the frequency of oscillation between pairs of states in response to some external driving function.

The dipole operator $-\mathbf{er}$ in (1.8) is the structure of the orbitals, which allows a separation of the expectation value in the preceding equation into radial and angular parts, $\langle 2 | \mathbf{r} \cdot \hat{\varepsilon} | 1 \rangle = \langle 2 | R | 1 \rangle \mathcal{I}$. Setting aside the radial part R , the angular integral \mathcal{I} can be written as a contraction over the spherical harmonic basis functions,

$$\mathcal{I} = \int_0^{2\pi} \int_0^\pi Y_{l_2, m_2}^*(\theta, \phi) \hat{\mathbf{r}} \cdot \hat{\varepsilon} Y_{l_1, m_1}(\theta, \phi) \sin \theta d\theta d\phi \quad (1.11)$$

which is zero unless some constraints, known as *selection rules*, are satisfied. To proceed, we assume that the atom is immersed in a magnetic field and define the z axis to be the direction of the magnetic field vector \mathbf{B} ⁵. The dipole operator can then be written as the superposition of the linear and circular oscillating field components,

$$\hat{\mathbf{r}} \cdot \hat{\varepsilon} \propto A_{\sigma-} Y_{1, -1} + A_z Y_{1, 0} + A_{\sigma+} Y_{1, +1}, \quad (1.12)$$

where the $A_{\sigma\pm}$ are the amplitudes of the clockwise- and anti-clockwise circular polarization, and A_z the amplitude of linear polarization in the atomic reference frame. When this expression is inserted into the integral \mathcal{I} , the orthogonality of spherical harmonics and the relationship

$$Y_{1, m} Y_{\lambda, \mu} = A Y_{1+\lambda, m+\mu} + B Y_{\lambda-1, m+\mu} \quad (1.13)$$

ensures

$$\Omega \propto a \delta_{l_2, l_1+1} \delta_{m_2, m_1+m} + b \delta_{l_2, l_1-1} \delta_{m_2, m_1+m} \quad (1.14)$$

where $m = \pm 1, 0$ as in the expansion of the dipole operator, and a, b are constants whose exact values are not required here. Thus $\mathcal{I} = 0$ unless $\Delta l = \pm 1$ and either $\Delta m_l = 0$ or

⁴This is a good approximation when the wavelength $\lambda = c/f$, fixed by the vacuum speed of light c , is much larger than the atom. This is universally applicable for our purposes as the size of the helium atom is $\approx 30\text{pm}$, some 0.1% of the shortest wavelength of light used in this thesis.

⁵This is true for almost all the contexts we encounter in this thesis, but where a magnetic axis is not present, one should perform an average over all angles as required.

$\Delta m_l = \pm 1$. Transitions not satisfying these conditions are said to be *forbidden*, but in reality they still occur, and can be accounted for by including higher terms in the series expansion of the interaction Hamiltonian. Emission or absorption events with $\Delta m_l = 0$ are called π -transitions, and correspond to the dipole moment induced by light with linear polarization along the quantization axis, whose amplitude is captured by the A_z term in Eqn. 1.12. The σ transitions couple to oscillations in the plane normal to the quantization axis, and correspond to transitions where $\Delta m_l = \pm 1$, driven by the $A_{\sigma\pm}$ terms.

This description of the coupling between atomic states and the electric field is sufficient, with some further work, to derive the Einstein rate equations for absorption and stimulated emission [21]. However, the more familiar phenomenon of spontaneous emission remains out of reach and requires the full-blown theory of quantum electrodynamics for an explanation, so we shall not proceed to derive it here. Instead we will have to be satisfied with a classical model which captures some of the essential features so far left unmentioned.

Classical oscillator model

In the *Lorentz oscillator* picture, one approximates an atom by a positive charge fixed at the origin with a harmonically-coupled negative charge with a single degree of freedom $x(t)$ whose potential is zero at $x(t) = 0$. The electron's equation of motion is $\ddot{x} + \Gamma\dot{x} + \omega_0^2 x = -eE(t)/m_e$, where

$$\Gamma = \frac{e^2 \omega^2}{6\pi\epsilon_0 m_e c^3} \quad (1.15)$$

is the damping rate corresponding to radiative decay. The spectrum of an exponentially decaying oscillator has the familiar Lorentzian lineshape,

$$\alpha(\omega) = \frac{6\pi\epsilon_0 c^3}{\omega_0^2} \frac{\Gamma}{\omega_0^2 - \omega^2 - i(\omega^3/\omega_0^2)\Gamma}, \quad (1.16)$$

where the polarizability $\alpha(\omega)$, whose quantum-mechanical origin is a central interest in Chapter ??, determines the amplitude of the dipole response via $\mathbf{p}(t) = \alpha(\omega)E(t)$. This response function features the characteristic full-width at half-maximum (FWHM) scale of each transition, which is the inverse of the lifetime $\tau = 1/\Gamma$. The interaction energy of the dipole and the electric field is $U_{dip} = -\frac{1}{2}\langle \mathbf{p} \cdot \mathbf{E} \rangle = -\frac{1}{2\epsilon_0 c} Re(\alpha)I(\mathbf{r})$, which inherits a spatial structure from the intensity $I(\mathbf{r})$. When the polarizability is positive (that is, when the light is red-detuned from ω_0 and the denominator has a positive real part) then the dipole oscillates in-phase with the field and so the interaction energy is minimized at the intensity maxima. This is the operational principle of optical dipole traps, wherein the *dipole force* $F_{dip} = -\nabla U_{dip} \propto \nabla I(\mathbf{r})$ therefore confines atoms to the focus of a red-detuned Gaussian beam⁶. Ashkin made the first demonstration of the dipole force by trapping micron-sized particles in 1970 [7]. Ashkin suggested 3D trapping of atoms in 1978 [8], and in 1986 Chu *et al.* accomplished the first optical trap of neutral atoms [17]. In 1987 Ashkin demonstrated optical trapping of single cells, viruses, and bacteria [6, 9], adding to the list of techniques propagated from physics labs into precision biology. The first BEC produced exclusively using optical trapping was achieved in 2001 [11]. Ashkin was awarded the Nobel prize in 2018 for his development of optical trapping. The dipole force is most pertinent to chapter ?? as it is the basic principle underpinning optical lattice traps, and to chapter ?? wherein the frequency at which $Re(\alpha) = 0$ is measured as a test of quantum electrodynamics.

In the case where the detuning Δ is small in comparison to ω_0 (as will be the case throughout this dissertation), the dipole potential can be written in the form [24]

$$U_{dip}(\mathbf{r}) = \frac{3\pi c^2}{2\omega_0^3} \frac{\Gamma}{\Delta} I(\mathbf{r}), \quad (1.17)$$

⁶The dipole force can also be generated with blue-detuned beams to create repulsive potential barriers, or confine atoms in the dark core of a blue-detuned Bessel beam

and absorption of light is captured by the imaginary part of the polarizability [21], which is related to the scattering rate as

$$\Gamma_{sc} = \frac{\text{Im}(\alpha)I(\mathbf{r})}{\hbar\epsilon_0 c}. \quad (1.18)$$

Light scattering competes with the dipole force because repeated absorption of photons with momentum $\hbar k$ at a rate Γ_{sc} gives rise to an effective force of $F_{sc} = \Gamma_{sc}\hbar k$, not to mention the deleterious effects of heating by repeated absorption events. Fortunately, in all situations relevant to our concerns here, the scattering rate can be written


$$\Gamma_{sc}(\mathbf{r}) = \frac{3\pi c^2}{2\hbar\omega_0^3} \left(\frac{\Gamma}{\Delta} \right)^2 I(\mathbf{r}), \quad (1.19)$$

from which it can be seen that $\Gamma_{sc}/U_{dip} \propto \Gamma/\Delta$ - that is, for large enough detuning, the scattering rate is dominated by the dipole force.

1.2 Helium

The idealized model of the hydrogen atom is fine for illustrating some important features of atomic physics, but in heavier atoms than Hydrogen⁷, interactions between electrons also play an important role, which is true even for the humble helium atom. Although the structure of helium is simple enough that theoretical calculations can confidently accrue many significant figures, with precision rivalling similar calculations for Hydrogen, the presence of a second electron does considerably complicate the physics⁸. The Helium Hamiltonian

$$\left(\frac{-\hbar^2}{2m} \nabla_1^2 + \frac{-\hbar^2}{2m} \nabla_2^2 + \frac{e^2}{4\pi\epsilon_0} \left(-\frac{Z}{r_1} - \frac{Z}{r_2} + \frac{1}{r_{12}} \right) \right) |\psi\rangle = E|\psi\rangle$$

for the two-electron wavefunction $|\psi\rangle$ includes kinetic terms $\propto \nabla_i^2|\psi\rangle$ and a central potential $\propto 1/r$ for each electron, plus a repulsive interaction inversely proportional to the electron separation r_{12} . The presence of a second electron also introduces another defining feature of quantum mechanics: spin. The electron wavefunctions must be antisymmetric under exchange of particle labels because all fermions obey the Pauli exclusion principle. On the other hand, the Hamiltonian is invariant under exchange of the electrons. If we denote the exchange operator by \hat{X} , then we have $[\hat{H}, \hat{X}] = 0$, implying \hat{X} and \hat{E} have the same eigenstates. Therefore the energy eigenbasis satisfies $\hat{X}|e\rangle = -|e\rangle$. 

It must be, then, that a given eigenstate must be ~~of the~~ separable into odd and even parts as either $|\psi\rangle = \psi_{space}^S \psi_{spin}^A$ or $|\psi\rangle = \psi_{space}^A \psi_{spin}^S$. We can enumerate the possibilities for the symmetric (spin) wavefunctions,

$$\psi_{spin}^S = |\uparrow\uparrow\rangle, \quad (1.20)$$

$$|\downarrow\downarrow\rangle, \quad (1.21)$$

$$(|\uparrow\downarrow\rangle + |\downarrow\uparrow\rangle)/\sqrt{2} \quad (1.22)$$

and the antisymmetric term

$$\psi_{spin}^A = (|\uparrow\downarrow\rangle - |\downarrow\uparrow\rangle)/\sqrt{2} \quad (1.23)$$

which are all degenerate in energy because the atomic Hamiltonian does not couple to the spin **sector**. For a singly-excited helium atom, as will always be the case in this thesis,

⁷Or as astronomers are wont to call them, ‘metals’

⁸As the old joke goes, atomic physicists count ‘one, two, many...’

the interaction term splits the spatial part of the wavefunction for a given set of quantum numbers into symmetric and antisymmetric forms

$$\psi_{space}^A = \frac{1}{\sqrt{2}} (u_{1s}(1)u_{nl} - u_{1s}(2)u_{nl}(1))$$

$$\psi_{space}^S = \frac{1}{\sqrt{2}} (u_{1s}(1)u_{nl} + u_{1s}(2)u_{nl}(1))$$

which furnish the spin wavefunctions to form the n^3L_J and n^1L_J states, referred to as (triplet) ortho- and (singlet) para-helium, respectively⁹. It can be shown via degenerate perturbation theory that the exchange antisymmetry produces the *exchange energy* difference between the singlet and triplet states, where the orthohelium state has a lower energy. The 2^3S_1 state, also denoted He^* , distinguishes helium amongst the zoo of atomic species available to the cold atom physicist by virtue of its 19.8 eV excitation energy and ≈ 7800 s lifetime [27]. This state is forbidden to decay to the ground state by the $\delta L \neq 0$ selection rule and also because the dipole operator does not couple states of different spin, such as the He^* state and the ground state. Decay to the ground state from the metastable state is therefore called *doubly forbidden*. Forbidden transitions can generally occur by higher-order interactions that are omitted from the dipole approximation, and the He^* state in particular can decay via a magnetic dipole transition. Nonetheless, the two-hour lifetime is effectively a ground state for the purposes of ultracold helium experiments, which generally last less than a minute. Fortuitously, the metastable state is connected to the 2^3P_2 state by a transition with a wavelength of 1083.331nm, which is far more readily accessible with compact laser systems than the ≤ 63 nm X-ray transitions from the true ground state. The 2^3P_2 state also provides an essentially closed transition cycle for laser cooling as its decay is dominated by transitions to the He^* state, obviating the need for complicated optical repumping schemes. There is also a forbidden transition to the true ground state, but as this decay is some billionfold slower, it is negligible for our purposes (nonetheless, it was measured in the ANU lab [26]).

The astute reader will notice the absence of presentation of an explicit form for the electron wavefunctions in the helium atom. Indeed, helium is not analytically solvable because its eigenfunctions are not separable into a form $\psi = \psi_1 \otimes \psi_2$. A variational approach is required for tractable and accurate calculations, which was developed by Hylleraas [29, 28, 30]. In the intervening century, numerical methods for calculating the energy levels and transition rates in the Helium atom have kept pace with precision experiments, and have incorporated the effects of relativity, nuclear recoil, and finite optical wavelength. A more detailed survey of recent progress is given in chapter ??.

Magnetic fields and the Zeeman effect

The inclusion of spin introduces another important feature of atomic spectra, the Zeeman effect, whose discovery heralded a ‘watershed’ moment of modern physics. The Zeeman effect refers to the phenomenon of spectral line splitting that occurs when an atom is immersed in a DC magnetic field. The interaction energy of an atom in a magnetic field,

$$H = -\boldsymbol{\mu} \cdot \mathbf{B} \quad (1.24)$$

has contributions from both orbital and spin angular momenta (\mathbf{L} and \mathbf{S} , respectively) through the atom’s magnetic moment

$$\boldsymbol{\mu} = -\mu_B \mathbf{L} - g_s \mu_B \mathbf{S}. \quad (1.25)$$

⁹In what follows, we use the spectroscopic convention and label states by the $n^{2S+1}L_J$, where $J = S + L$ because the helium nucleus is spinless, and we drop the $(1s)$ term as the second electron will invariably be in the ground state in all cases we consider - Doubly-excited helium is highly unstable because the first excited state (19.8eV) has about 80% of the ionization energy of Helium (25.4eV).

Working in the $|LSJm_J\rangle$ basis, where J and m_J are the total angular momentum and its z-projection, yields the eigenenergies $E_Z = g_J \mu_B B$. The atomic g-factor can be written as

$$g_J = \frac{3}{2} + \frac{S(S+1) - L(L+1)}{2J(J+1)}, \quad (1.26)$$

using the approximate value of the electron g-factor $g_s = 2$. The eigenstates of the field-free atomic Hamiltonian will be $2J + 1$ -fold degenerate and specified by the $|Lm_LSm_S\rangle$ quantum numbers. Adding the magnetic field interaction breaks this degeneracy and leads to the Zeeman splitting. The field-free and magnetic-interaction terms can be written in a common basis in terms of the Clebsch-Gordan coefficients and then diagonalized, as described in chapter ???. The aforementioned anomalous Zeeman effect arises in triplet states because the inter-level spacing depends on m and g_J , which splits spectral lines as well as levels, whereas singlet states have $g_J = 1$ and transitions between them do not fan out in the same fashion.

The classical dipole envisions only circular polarization is visible along the quantization axis (z oscillation is not visible), but from transverse directions one can see the z oscillation and also the one-dimensional oscillations (eg along x when viewing the y axis) - so in a spatially varying mag field... And we're nearly at the point of being able to project the Stokes vectors into the local field

For all the intricacy of atomic structure, life would be very dull indeed were it not for the interactions between them. Indeed, the material reality of the world depends, in a sense, less on the structure of its building blocks and more on how they fit together¹⁰. The varied and central roles of interactions will be revisited in later chapters, traversing the spectrum from isolated, to weakly-interacting, to distinctly many-body systems.

1.3 Interacting atoms

Here we briefly review elastic scattering, and then turn to important inelastic scattering processes present in our experiments. A detailed primer in atomic scattering physics can be found in the classic texts [49] and [48], with more detail in the latter. An exhaustive review of low-temperature scattering studies up to the turn of the millenium can be found in [64]. I focus here on two-body collisions, which are the dominant interactions in the low-density regime of ultracold helium. Low densities imply that low temperatures are required to achieve high phase space density and reach the degenerate regime, which are necessary conditions to minimize the two-body loss processes characteristic to metastable helium. Two-body collisions are also the crucial enabler for thermalization during the evaporative cooling employed to reach such low temperatures, so long as the relaxation times are shorter than the sample lifetime.

Neglecting spin-orbit and relativistic effects the two-body scattering problem reduces to the Keplerian Schrödinger equation in the centre-of-momentum frame,



$$\left(\frac{\hbar^2}{2m^*} \Delta + V(r) - E \right) \psi(r) = 0, \quad (1.27)$$

where ψ is the wavefunction capturing the relative motion of the two atoms in terms of the separation $r = |\mathbf{r}_1 - \mathbf{r}_2|$ between the particles and the reduced mass $m^* = m_1 m_2 / (m_1 + m_2)$. In the asymptotic regime where r is much larger than the scale of $V(r)$, the solution takes the form of a superposition of the initial plane wave and the scattered solution,

$$\psi(r) \propto e^{ikz} + f(\theta) \frac{e^{ikr}}{r}, \quad (1.28)$$

¹⁰This could be said to underpin the transferability of systems from a natural instantiation to analytic or simulated contexts, because there is truth in the *structure* which is independent of the *substrate*.

where $k = \sqrt{2m^*E}/\hbar$ is the plane wave-vector of the initial approach and θ is the angle from the direction of incidence. A general solution can be found by expanding $f(\theta)$ into a convenient basis of *partial waves* (spherical harmonics) which are labeled s, p, d, f, \dots in order of increasing angular momentum. In the low-energy limit, $f(\theta)$ is independent of angle and only the spherically symmetric s-wave term contributes, and the limit $f(\theta) \rightarrow -a$ is accordingly called the s-wave scattering length. In the millikelvin regime the scattering physics is determined by just a few partial waves [40], and in the ultracold (microkelvin or colder) regime only the s-wave scattering channel is significant. The total cross section $|f(\theta)|^2/|\psi|^2$, which is the total probability that a near collision results in particle scattering approaches $\sigma = 8\pi a^2$ for polarized bosons¹¹ [51].

The s-wave scattering length is also an important determinant of the energetics of degenerate matter such as BEC. Because BECs are dominated by long-wavelength behaviour, a theoretical treatment can be considerably simplified by considering only the *effective interactions*. By formulating the scattering problem in momentum space, the effective interaction strength for low-energy scattering $g = 4\pi\hbar^2 a/m$, also referred to as the pseudopotential, can be found by integrating out the high-frequency modes (also known as the Born approximation). This necessarily washes out extremely short-range correlations but makes fairly accurate calculations much more tractable by reducing the size of the basis set used in a calculation.

In molecular collisions the scattering process will obviously depend on the relative orientation of the molecules. In collisions between single atoms, though, there is a more subtle orientation-dependence which arises from the total spin of the two-particle system. The three possible configurations between pairs of He* atoms correspond to the singlet $^1\Sigma_g^+$, triplet $^3\Sigma_u^+$, and quintet $^5\Sigma_g^+$ Born-Oppenheimer molecular potentials¹², with total spin 0, 1, and 2. When the atoms are spin-polarized, as they are when confined in magnetic traps, then the only scattering that occurs is in the quintet channel. In low-energy scattering contexts dominated by s-wave scattering, odd partial waves do not contribute to the interaction potential and hence the triplet $^3\Sigma_u^+$ potential is dominated by the quintet $^5\Sigma_g^+$ term for all interactions with nonzero total spin [35]. As such the inter-species scattering lengths $a_{1,1}$, $a_{1,0}$, $a_{1,-1}$, and $a_{-1,-1}$ are all equal [35, 62]. The most accurate determination of the s-wave scattering length in these configuration is 7.512 nm [42], in agreement with calculations performed the year before the measurements [51]. When the total spin is zero, the singlet term contributes and so $a_{1,-1} \approx 8.8$ nm and $a_{0,0} \approx 3.8$ nm [35, 62]. In general this thesis will be concerned with interactions between spin-polarized helium atoms and hence will use the abbreviation $a \equiv a_{1,1}$ unless specified otherwise.


A powerful tool available in some cold atom experiments are Feshbach resonances¹³. A detailed description is found in [16], but from an operational standpoint they allow control of the scattering length as $a = \tilde{a}(1 - \Delta/(B - B_0))$, where B is the strength of an ambient magnetic field, B_0 is the resonance value of the field, \tilde{a} is the value when the field is far from a resonance and Δ sets the resonance width. The scattering length can thus be tuned in size and even in sign. Fundamentally, the stability of a BEC requires a positive s-wave scattering length¹⁴, and switching from stable to unstable configurations permits one to examine condensate collapse (as in the spectacular Bosenova experiments [papers]) and also to explore the BEC-BCS crossover [papers]. The spinless nucleus of ^4He prohibits coupling of bound states within an m_J manifold from crossing an open-channel threshold, precluding this pathway to a Feshbach resonance [23]. Nonetheless, Feshbach resonances

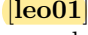
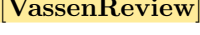
¹¹For fermion pairs with odd total spin, the cross section tends to zero because of the Pauli exclusion principle, and thus the s-wave scattering length vanishes.

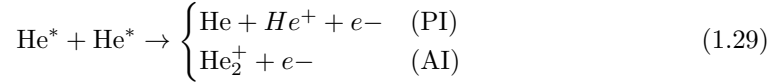
¹²the subscript g and u are short for *gerade* and *ungerade* (German for even and odd) label the reflection symmetry of the two-body wavefunction.




¹³Feshbach resonances originated in Feshbach's work in nuclear physics (Feshbach 1958, 1962) and Fano worked on in atomic context (fano 1961), but these fano-feshbach resonances are referred to in general as feshbach resonances.

¹⁴Although in some negative-temperature states created in an optical lattice, a BEC can be stable even with attractive interactions [15]

induced by spin-spin interactions between helium atoms have been predicted [63, 23], but have not observed to date [14]. In a forthcoming work, the authors (including members of the ANU He* lab) describe calculations with a newer method predicting, unfortunately, the absence of Feshbach resonances between ^4He - ^4He collisions .

Inelastic scattering processes are those which exchange energy between the internal and motional states of either atom. They can be represented as a complex scattering potential  which permits losses from on-shell scattering channels. An important inelastic process characteristic of metastable noble gases  is *Penning ionization*. This can occur through the decay channels



wherein the first channel is formally called Penning ionization and the second is Auto-ionization and the rate of the latter is generally very small in comparison to the former [36]. Indeed, the energy of the metastable state is sufficient to ionize any neutral atom (except helium or neon) from its ground state, and underpins the single-atom sensitivity of our solid state detector (described in section ??). Aside from attracting intensive study in its own right [46, 57, 40], this explosive potential was a significant hurdle for researchers attempting to achieve Bose-Einstein condensation with helium.  The density achieved in early magneto-optical traps (MOTs) was limited to some hundredfold less than the alkali-metal MOTs of the day [10, 34, 39]. Helium MOT densities were limited by losses through two-body collisions involving atoms in the 2^3S_1 and those excited to the 2^3P_2 state by the trapping beams, as opposed to rescattering pressure as in the case of alkali metals. Indeed, while the Penning loss rate constant ¹⁵ between pairs of 2^3S_1 atoms is of order $2 \times 10^{-9} \text{ cm}^3/\text{s}$, the loss rate for $2^3S_1 - 2^3P_2$ collisions is around $10^{-7} \text{ cm}^3/\text{s}$. Thus early MOTs had loss rates which were a population-weighted average of these rates, around $7 \times 10^{-8} \text{ cm}^3/\text{s}$ [64]. Such light-assisted losses limited the population achievable in MOTs until larger beams and detunings were used [60]. These reduced Penning ionization rates to the order of $5 \times 10^{-9} \text{ cm}^3/\text{s}$ at large detunings.  In the dark, the rate constant is an order of magnitude or so lower again [39], but the process is still too fast to permit access to magnetic traps of sufficient lifetime and density to reach degeneracy. Fortunately, the inelastic scattering cross-sections depend on the molecular potentials in such a way that condensation becomes attainable: When all the atoms are polarized in the either of the $m_J = \pm 1$ states, the incoming state has a total spin of 2, whereas the reaction products have a total spin of 1, and so this process is forbidden. In reality, it does occur through a weak virtual spin-dipole transition [55], but slowly enough that spin-polarized He^* exhibits a 10^4 -fold reduction in  ionization rate. At field strengths above 50G, however, the suppression weakens [55, 14]. Other noble gases also exhibit highly energetic metastable states, but the lifetime and suppression of Penning ionization decreases with increasing mass [43, 44]. Thus Helium may be the only noble gas ever to be Bose-condensed.

1.4 Bose-Einstein condensation

The ‘fifth state of matter’¹⁶ has a long and storied history[2]. Interest in BEC was amplified back in the middle of the 20th century when Fritz London proposed that Bose-Einstein condensation was connected to the superfluid phenomenon in liquid helium. Nikolay Nikolayevich Bogolyubov formalized this connection and so, historically speaking, helium was

¹⁵The rate constant $\beta_{i,j}$ for losses via collisions between atoms in states i and j yields an absolute loss rate per volume per time through the product with the respective densities, $\Gamma_{i,j} = \beta_{i,j} n_i n_j \text{ cm}^{-3}\text{s}^{-1}$.

¹⁶The familiar first phases, solid, liquid, and gas, are vanishingly rare in cosmological terms. The fourth, plasma, is the state of at least 99% of the ordinary matter in the universe [1]. Helium comprises about 23%, most of which being primordial baryons formed during the recombination epoch.

the element which hosted the earliest experimental realization of Bose-Einstein condensation, albeit with a very small condensed fraction¹⁷. While liquid helium is a rare thing in cosmological terms, BEC may have existed already for millions of years in the superdense quark matter of neutron stars [25, 38, 12, 45], wresting the claim of cosmic novelty from human hands. Nonetheless, the essentially pure atomic condensates and the emerging study of molecular condensates in laboratory settings are among the most extreme conditions in the universe, and are not believed to occur naturally elsewhere in the universe. Following the oft-cited seven decades between the initial theoretical descriptions and the experimental realization of atomic Bose-Einstein condensates (BEC) [anderson95, 20, 52], the field has become quite industrious at the eve of its centenary. As pithily put by a review only five years after the Nobel-winning experiments, ‘Any attempt to review recent progress is out of date as soon as it is published’ [18]. This is no less true today, as the number of ultracold quantum gas experiments worldwide now number nearly 200¹⁸ and numerous companies have been founded on the promise of selling better sensors and computers using technologies based on BEC physics. There are numerous treatments of the theory of Bose-Einstein condensation, for example the classic textbooks [49, 48] and review articles [19, 65, 18]. The essential background for discussion here draws on these standard sources unless otherwise cited.

As for what a BEC *is*, there are several workable operational definitions, but a precise and lab-relevant definition is surprisingly elusive. The canonical description of Bose-Einstein condensation is the condition where the de Broglie wavelength associated with thermal kinetic energy

$$\lambda_T = \frac{h}{\sqrt{2\pi m k_B T}} \quad (1.30)$$

is comparable to the interparticle spacing, coinciding with a macroscopic occupation of the single-particle ground state as the de Broglie waves of many bosons constructively interfere. This condition can also be restated as the point when the phase space density

$$\mathfrak{N} = n\lambda_T^3 \quad (1.31)$$

exceeds the critical value of $\zeta(3) \approx 2.612$. This is generally introduced as the point where the volume over which the atoms are ‘delocalized’ exceeds the average volume per particle, and so the spin-statistics of the particles dictate the deviation from the statistics of an ideal gas. Although it is commonly said that at this point the ‘wavefunctions overlap’, the wavefunctions of the individual particles in a trapped gas overlap wherever the wavefunction is supported - that is, throughout the trap. Furthermore, the de Broglie wavelength pertains to the wavelength associated with the plane-wave motion of a free particle rather than the spatial scale of the ‘wavepacket’ of a particle, and as given above is defined as the wavelength corresponding to the *average* particle velocity, rather than fully characterizing the ensemble. Thus even above the critical temperature there are many states with long wavelengths who will be populated, and so the ‘delocalization’ picture is not so sharp. A more precise criterion is to compute, in the framework of the grand canonical ensemble, the number of particles in the ground state. For a Bose gas this yields

$$0N_0 = \frac{1}{\exp((E_0 - \mu)/k_B T) - 1}, \quad (1.32)$$

where E_0 is the ground state energy of the single-particle Hamiltonian and μ is the chemical potential of an adjoining reservoir. One can then show that, above the critical temperature T_c , the ground-state population diverges, corresponding to Bose-Einstein condensation.

¹⁷Nikolay was a darling of Russian theoretical physics, receiving his PhD-equivalent qualification at 19 and made important contributions to quantum field theory. In his famous paper on the problem of interacting bosons, his name is transliterated as *Bogolubov*. Bogolyubov and *Bogoliubov* are also common transliterations.

¹⁸See everycoldatom.com

However, in laboratory realizations of BEC, there is no reservoir attached to the system under study, but rather an isolated gas at some finite entropy which contains both the thermal and condensed fractions (if the latter is present).

Moreover, in the presence of interactions, these criterion faces another issue: the stationary states of an interacting gas of N atoms cannot be written as a **product** $|\Psi\rangle = |\psi_i\rangle^{\otimes N}$ of single-particle eigenstates $|\psi_i\rangle$. That is, while measurements are confined to observables of single particles, the single-particle states are not eigenstates and so it is not sensible to talk of their ‘macroscopic occupation’. The Penrose-Onsager criterion [47] provides an alternative in terms of the density matrix ρ for the isolated composite system comprised of all the gas particles. The single-particle density matrix is then the expected value of the one-body field operator

$$\rho^{(1)} = \text{Tr} \left(\rho \hat{\Psi}^\dagger \hat{\Psi} \right), \quad (1.33)$$

whose eigenvalues p_l^1 give the occupation probability of the l^{th} eigenvector of $\rho^{(1)}$. The eigenvectors themselves are the single-particle modes. If any eigenvalue p_l^1 is proportional to N in the limit $N \rightarrow \infty$, then the system is said to have undergone Bose-Einstein condensation (or, simply, *condensed*) into the l^{th} mode. Of course, real systems are subject to atom losses and heating, violating the assumptions of equilibrium underpinning both the approaches above.

This is all to illustrate the point that the real world is full of intricacies and the ‘intuitive’ pictures of BEC, despite being useful pedagogical tools, can skirt around some important physical features. Ultimately though, this is a thesis concerned with experiments, and we shall say little more than remarking on the compelling agreement between theoretical and actual condensates irrespective of the preceding issues. Indeed, the Penrose-Onsager criterion has been shown to be a good characterization of a non-Hermitian polariton condensate [37] in that off-diagonal long range order (i.e. phase coherence) emerges along with the growth of a single eigenvalue of the one-body density matrix. As the saying goes, if it interferes like a condensate [4], undergoes number fluctuations like a condensate [33], has HBT correlations like a condensate [53, 31], Kibble-Zureks like a condensate [5], and quacks like a condensate [3], then it probably *is* a condensate.

While most atomic condensates, and all of those in this thesis, are trapped in non-uniform potentials, many important features of condensates are easier to state for homogeneous systems. One can usually extend calculations to harmonically trapped systems by a local density approximation, wherein one performs a density-weighted average across a condensate, considering each volume element as a homogenous condensate in its own right. Thus, for the most part the following discussion will focus on homogeneous systems for simplicity’s sake. I present some particular results in the case of a harmonically trapped gas at the end of this section.

Bogoliubov theory

The fundamental theoretical object of interest is the Hamiltonian of a bosonic quantum field with two-body interactions,

$$\hat{H} \int \left(\frac{\hbar^2}{2m} \nabla \hat{\Psi}^\dagger(\mathbf{r}) \nabla \hat{\Psi}(\mathbf{r}) \right) d\mathbf{r} + \frac{1}{2} \int \left(\hat{\Psi}^\dagger(\mathbf{r}') \hat{\Psi}^\dagger(\mathbf{r}) V(\mathbf{r}' - \mathbf{r}) \hat{\Psi}(\mathbf{r}') \hat{\Psi}(\mathbf{r}) \right) d\mathbf{r}' d\mathbf{r} \quad (1.34)$$

where $\Psi(r)$ are the field operators subject to the bosonic commutation relations

$$[\Psi(r), \Psi^\dagger(r')] = \delta(r - r') \quad (1.35)$$

$$[\Psi^\dagger(r), \Psi^\dagger(r')] = [\Psi(r), \Psi(r)] = 0. \quad (1.36)$$

We can then write the field operator in the suggestive form

$$\hat{\Psi} = \psi_0 \hat{a}_0 + \sum_{i \neq 0} \psi_i \hat{a}_i \quad (1.37)$$

in terms of an orthonormal basis of single-particle modes ψ_i and corresponding field operators \hat{a}_i . In doing so we distinguish $\mathbf{p} = 0$ as the condensed mode, and say that condensation occurs when $N_0 = \langle \hat{a}_0^\dagger \hat{a}_0 \rangle = \mathcal{O}(N)$. The observation that the condensed mode has a population of order N means that in the thermodynamic limit ($N \rightarrow \infty$, $V \rightarrow \infty$), one particle here or there will not really make a measurable difference. This heuristic can be expressed quantitatively as the Bogoliubov approximation wherein the annihilation and creation operators for the condensed mode are replaced with complex numbers as per

$$\hat{a}_0 = \sqrt{N_0} e^{i\alpha}, \hat{a}_0^\dagger = \sqrt{N_0} e^{-i\alpha}, \quad (1.38)$$

which permits the condensate wavefunction to take the form

$$\hat{\Psi} = \sqrt{N_0} e^{i\alpha} \psi_0 + \delta\hat{\Psi} \quad (1.39)$$

$$= \Psi_0 + \delta\Psi \quad (1.40)$$

The first term is the condensate wavefunction (the *mean-field* term), and the second corresponds to the population of non-condensed modes thanks to the effect of interactions, which are captured by the quasiparticle picture sketched in the next section. The emergence of a condensate has many of the hallmarks of a classical phase transition: kinetic effects are necessary to redistribute energy and reach steady-state; a unique critical temperature T_c exists; below T_c an *order parameter* takes on a nonzero value; and condensation is equivalent to the spontaneous breaking of a $U(1)$ gauge symmetry [66]. Above the critical temperature, $N_0 = 0$, and in general it exhibits a discontinuous derivative at the critical temperature. Hence, in the Landau-Ginzburg framework, condensation is a second-order phase transition¹⁹. The other hallmark of Landau-Ginzburg phase transitions is the spontaneous breaking of symmetry as one crosses from the disordered to the ordered phase (as when a solid breaks the translational symmetry of the fluid phase). Condensates do exhibit such symmetry breaking: The Hamiltonian has a $U(1)$ gauge symmetry, but the ground state of a condensate spontaneously chooses a fixed but unpredictable phase α . By interfering two independently prepared condensates, one observes interference fringes [4], and indeed, the fringe locations will change with each realization and measurement. More directly, one can interfere light leakage from a reservoir-coupled photon condensate against a reference beam, and observe that phase jumps occur in the output when the condensate field drops to zero. That is, the re-emergence of the condensate is heralded by the selection of a new, specific, phase, apparently uncorrelated with the phase that existed before it [54].

Symmetry breaking is a subtle point discussed infrequently in standard textbooks. It happens that one can substitute complex numbers for the field operators, even when $\langle N_0 \rangle \rightarrow 0$ and still obtain correct results [22]. That is, condensation is not necessary for the Bogoliubov approximation to be valid. However, it *is* the case that the onset of condensation coincides with the ground state breaking²⁰ the $U(1)$ symmetry [58].

Harmonically trapped condensates

Turning back toward harmonic gases, we can begin from the full Hamiltonian (Eqn. (1.34)) and produce an effective Schrödinger equation. By assuming slow variations in the density, integrating out short-wavelength modes as in the Born approximation, one can derive the Gross-Pitaevskii equation (GPE),

$$-\hbar\partial_t\Psi_0(r,t) = \left(-\frac{\hbar^2\nabla^2}{2m} + V(r,t) + g|\Psi_0(r,t)|^2\right)\Psi_0(r,t). \quad (1.41)$$

¹⁹In the Ehrenfest picture one is instead concerned with the number of times one must differentiate some state function (e.g. specific heat, compressibility, pressure, free energy) before finding a discontinuity at the critical point. In this picture, the transition is first-order as one has continuous state functions with discontinuous derivatives.

²⁰This is sometimes called ‘breaking the gauge symmetry’. This is a misnomer, as a gauge symmetry is a property of the theory, not a state, and all consistent theories must be gauge symmetric throughout. These subtleties are discussed at length in lucid terms in [50].

which is valid for arbitrary interactions dominated by the s-wave scattering length. If one further assumes that the condensate density varies on scales larger than the healing length $\xi = \hbar/\sqrt{2mgn}$, one can make the Thomas-Fermi approximation and ignore the kinetic term in the GPE, whereby the condensate density profile can be written as

The importance can be seen by noting that

$$n(\mathbf{r}) = \frac{\mu - V(\mathbf{r})}{g}, \quad (1.42)$$

where μ is the chemical potential. The chemical potential for the harmonically trapped condensate also fixes the average energy per particle:

$$\mu = \frac{\hbar\bar{\omega}}{2} \left(\frac{15Na}{a_{ho}} \right)^{2/5} = \frac{7}{5} \frac{E}{N} \quad (1.43)$$

For a Bose gas confined in a harmonic potential of the form

$$V = \frac{1}{2}m\omega_x^2x^2 + \frac{1}{2}m\omega_y^2y^2 + \frac{1}{2}m\omega_z^2z^2, \quad (1.44)$$

the condition $\mu - V(\mathbf{r}) = 0$ determines the boundary of the condensate, giving the Thomas-Fermi radii $R_i = \sqrt{2\mu/m\omega_i^2}$, where $i \in \{x, y, z\}$. This produces the famous inverted-parabola density profile with a peak density of

$$n_0 = \frac{1}{8\pi} \left((15N_0)^2 \left(\frac{m\bar{\omega}}{\sqrt{a\hbar}} \right)^6 \right)^{1/5}. \quad (1.45)$$

The Thomas-Fermi approximation is valid when $Na/a_{ho} \gg 1$, where $a_{ho} = \sqrt{\hbar/m\bar{\omega}}$ is the length scale of the ground state of the harmonic oscillator. This is when the mean-field energy significantly outweighs the kinetic term. The phase space density for condensation is achieved at the (ideal) critical temperature

$$T_c^0 = \frac{\hbar\bar{\omega}}{k_B} \left(\frac{N}{\zeta(3)} \right)^{1/3} \quad (1.46)$$

$$\approx 0.94 \frac{\hbar\bar{\omega}N^{1/3}}{k_B}. \quad (1.47)$$

where $\bar{\omega} = (\omega_x\omega_y\omega_z)^{1/3}$ is the geometric mean of the trapping frequencies, and the condensed fraction below the critical temperature is

$$\frac{N_0}{N} = 1 - \left(\frac{T}{T_c^0} \right)^3. \quad (1.48)$$

The rest of the population, occupying excited single-particle states, is called the thermal fraction. The population N_T of the thermal fraction saturates as $\frac{N_T}{N} = \left(\frac{k_B T}{\hbar\bar{\omega}} \right)^3$, wherein any atoms added to the gas fall into the condensate mode, regardless of the density of the gas. Real gases generally don't show such a feature, and this bifurcation is corrected by including the effect of interactions on the thermodynamics of the Bose gas. Interactions between particles reduce the critical temperature in a harmonic trap, which can be understood in terms of repulsive interactions reducing the density at a given temperature and thus requiring a lower temperature to achieve a given n . The resulting shift in the critical temperature can be supplemented with a correction for the finite size of the condensate and written as

$$\frac{\delta T_c}{T_c^0} = -1.3 \frac{a}{a_{ho}} N^{1/6} - 0.73 \frac{\langle \omega \rangle}{\omega_{ho} N^{1/3}} \quad (1.49)$$

where the latter term, the correction for finite atom number, includes the arithmetic mean trapping frequency $\langle\omega\rangle$ and vanishes in the thermodynamic limit ($N \rightarrow \infty$, $V \rightarrow \infty$, N/V finite). These deviations from ideal behaviour have been observed in experiments [59, 56].

As for the practical production of condensates, much quality literature has been written on the theory and techniques of atomic cooling techniques employed to reach degeneracy. These days, such techniques are standard across hundreds of laboratories and so space will not be spared for their general consideration here. The curious reader is directed to [32, 18, 41, 61] for detailed discussions. Rather, in the next chapter I discuss the specifications of the apparatus used in the course of this research to implement the general principles of atomic cooling and trapping to achieve condensation.

Bibliography

- [1] A list of sources is found at plasma-universe.com.
- [2] See <https://www.bose.res.in/Conferences/BECRP18/Mukunda.pdf> and references therein.
- [3] Admittedly, to my knowledge, this has yet to be detected.
- [4] M R Andrews et al. “Observation of Interference Between Two Bose Condensates”. In: *Science* 275 (1997), pp. 637–641.
- [5] M. Anquez et al. “Quantum Kibble-Zurek Mechanism in a Spin-1 Bose-Einstein Condensate”. In: *Physical Review Letters* 116.15 (2016), p. 155301. ISSN: 0031-9007, 1079-7114. DOI: 10.1103/PhysRevLett.116.155301.
- [6] A Ashkin, J. M. Dziedzic, and T. Yamane. “Optical trapping and manipulation of single cells using infrared laser beams”. In: *Nature* 330 (1987). DOI: <https://doi.org/10.1038/330769a0>.
- [7] A. Ashkin. “Acceleration and Trapping of Particles by Radiation Pressure”. In: *Phys. Rev. Lett.* 24 (4 Jan. 1970), pp. 156–159. DOI: 10.1103/PhysRevLett.24.156. URL: <https://link.aps.org/doi/10.1103/PhysRevLett.24.156>.
- [8] A. Ashkin. “Trapping of Atoms by Resonance Radiation Pressure”. In: *Phys. Rev. Lett.* 40 (12 Mar. 1978), pp. 729–732. DOI: 10.1103/PhysRevLett.40.729. URL: <https://link.aps.org/doi/10.1103/PhysRevLett.40.729>.
- [9] A. Ashkin and J. M. Dziedzic. “Optical trapping and manipulation of viruses and bacteria”. In: *Science* 235 (1987). DOI: 10.1126/science.3547653.
- [10] F Bardou et al. “Magneto-Optical Trapping of Metastable Helium: Collisions in the Presence of Resonant Light”. In: *Europhysics Letters* 20 (1992). URL: <https://iopscience.iop.org/article/10.1209/0295-5075/20/8/003/>.
- [11] M. D. Barrett, J. A. Sauer, and M. S. Chapman. “All-Optical Formation of an Atomic Bose-Einstein Condensate”. In: *Phys. Rev. Lett.* 87 (1 June 2001), p. 010404. DOI: 10.1103/PhysRevLett.87.010404. URL: <https://link.aps.org/doi/10.1103/PhysRevLett.87.010404>.
- [12] Gordon Baym, Christopher Pethick, and David Pikes. “Superfluidity in Neutron Stars”. In: *Nature* 224.5220 (Nov. 1969), pp. 673–674. ISSN: 0028-0836, 1476-4687. DOI: 10.1038/224674a0. URL: <http://www.nature.com/articles/224674a0>.
- [13] James Binney and David Skinner. *The Physics of Quantum Mechanics*. Capella Archive, 2008.
- [14] J. S. Borbely et al. “Magnetic-field-dependent trap loss of ultracold metastable helium”. In: *Phys. Rev. A* 85 (2 Feb. 2012), p. 022706. DOI: 10.1103/PhysRevA.85.022706. URL: <https://link.aps.org/doi/10.1103/PhysRevA.85.022706>.
- [15] S Braun et al. “Negative absolute temperature for motional degrees of freedom”. In: *Science* 399 (2013). DOI: 10.1126/science.1227831.

- [16] Cheng Chin et al. “Feshbach resonances in ultracold gases”. In: *Rev. Mod. Phys.* 82 (2 Apr. 2010), pp. 1225–1286. DOI: 10.1103/RevModPhys.82.1225. URL: <https://link.aps.org/doi/10.1103/RevModPhys.82.1225>.
- [17] Steven Chu et al. “Experimental Observation of Optically Trapped Atoms”. In: *Phys. Rev. Lett.* 57 (3 July 1986), pp. 314–317. DOI: 10.1103/PhysRevLett.57.314. URL: <https://link.aps.org/doi/10.1103/PhysRevLett.57.314>.
- [18] Ph. W. Courteille, V. S. Bagnato, and V. I. Yukalov. “Bose-Einstein Condensation of Trapped Atomic Gases”. In: (2001). eprint: [cond-mat/0109421](https://arxiv.org/abs/cond-mat/0109421).
- [19] Franco Dalfovo et al. “Theory of Bose-Einstein condensation in trapped gases”. In: *Rev. Mod. Phys.* 71 (3 1999), pp. 463–512. DOI: 10.1103/RevModPhys.71.463. URL: <https://link.aps.org/doi/10.1103/RevModPhys.71.463>.
- [20] K B Davis et al. “Bose-Einstein condensation in a gas of sodium atoms”. In: *Physical Review Letters* 75 (1995), pp. 3969–3973. DOI: <https://doi.org/10.1103/PhysRevLett.75.3969>.
- [21] C J Foot. *Atomic Physics*. Oxford university press, 2005.
- [22] J Ginibre. “On the asymptotic exactness of the Bogoliubov approximation for many boson systems”. In: *Communications in Mathematical Physics* 8 (1967), pp. 26–51. DOI: 10.1007/BF01646422.
- [23] M. R. Goosen et al. “Feshbach resonances in $^3\text{He}^*$ - $^4\text{He}^*$ mixtures”. In: *Phys. Rev. A* 82 (4 Oct. 2010), p. 042713. DOI: 10.1103/PhysRevA.82.042713. URL: <https://link.aps.org/doi/10.1103/PhysRevA.82.042713>.
- [24] Rudolf Grimm, Matthias Weidemüller, and Yurii B. Ovchinnikov. “Optical Dipole Traps for Neutral Atoms”. In: ed. by Benjamin Bederson and Herbert Walther. Vol. 42. *Advances In Atomic, Molecular, and Optical Physics*. Academic Press, 2000, pp. 95–170. DOI: [https://doi.org/10.1016/S1049-250X\(08\)60186-X](https://doi.org/10.1016/S1049-250X(08)60186-X). URL: <http://www.sciencedirect.com/science/article/pii/S1049250X0860186X>.
- [25] B. Haskell and A. Sedrakian. “Superfluidity and Superconductivity in Neutron Stars”. In: *The Physics and Astrophysics of Neutron Stars*. Ed. by L Rezzolla et al. *Astrophysics and Space Science Library*, 2018, pp. 401–454. DOI: https://doi.org/10.1007/978-3-319-97616-7_8.
- [26] S. S. Hodgman et al. “Complete ground-state transition rates for the helium 2^3P manifold”. In: *Phys. Rev. A* 80 (4 Oct. 2009), p. 044501. DOI: 10.1103/PhysRevA.80.044501. URL: <https://link.aps.org/doi/10.1103/PhysRevA.80.044501>.
- [27] S. S. Hodgman et al. “Metastable Helium: A New Determination of the Longest Atomic Excited-State Lifetime”. In: *Physical Review Letters* 103.5 (July 2009). DOI: 10.1103/physrevlett.103.053002. URL: <http://dx.doi.org/10.1103/PhysRevLett.103.053002>.
- [28] E A Hylleraas. “Neue berechnung der Energie des Heliums im Grundzustande, sowie des tiefsten Terms von Ortho-helium”. In: *Z Physik* (54 1929).
- [29] E A Hylleraas. “Über den grundzustand des Heliumatoms”. In: *Z Physik* (48 1920).
- [30] E A Hylleraas and B Undheim. “Numerische berechnung der 2S terme von Ortho- und Par-helium”. In: *Z Physik* (65 1930).
- [31] T Jelte et al. “Comparison of the Hanbury Brown-Twiss effect for bosons and fermions”. In: *Nature* 445 (2007). DOI: [doi:10.1038/nature05513](https://doi.org/10.1038/nature05513).
- [32] W. Ketterle, D. S. Durfee, and D. M. Stamper-Kurn. “Making, probing, and understanding Bose-Einstein condensates”. In: (1999). eprint: [cond-mat/9904034](https://arxiv.org/abs/cond-mat/9904034).

- [33] M. A. Kristensen et al. “Observation of Atom Number Fluctuations in a Bose-Einstein Condensate”. In: *Phys. Rev. Lett.* 122 (16 Apr. 2019), p. 163601. DOI: 10.1103/PhysRevLett.122.163601. URL: <https://link.aps.org/doi/10.1103/PhysRevLett.122.163601>.
- [34] M Kumukura and N Morita. “Magneto-Optical trap of metastable helium-3 atoms”. In: *Applied Physics B* 46 (2000). DOI: <https://doi.org/10.1007/s003400050861>.
- [35] P. J. Leo et al. “Ultracold collisions of metastable helium atoms”. In: *Phys. Rev. A* 64 (2000), p. 042710. DOI: 10.1103/PhysRevA.64.042710.
- [36] Müller M.W. et al. “Experimental and theoretical studies of the Bi-excited collision systems $\text{He}^*(23\text{ S}) + \text{He}^*(23\text{ S}, 21\text{ S})$ at thermal and subthermal kinetic energies”. In: *Zeitschrift für Physik D Atoms, Molecules and Clusters* (21 1991), pp. 89–112. DOI: <https://doi.org/10.1007/BF01425589>.
- [37] F. Manni et al. “Penrose-Onsager Criterion Validation in a One-Dimensional Polariton Condensate”. In: *Phys. Rev. Lett.* 109 (15 2012), p. 150409. DOI: 10.1103/PhysRevLett.109.150409. URL: <https://link.aps.org/doi/10.1103/PhysRevLett.109.150409>.
- [38] Noël Martin and Michael Urban. “Superfluid hydrodynamics in the inner crust of neutron stars”. In: *Phys. Rev. C* 94.6 (Dec. 2016), p. 065801. ISSN: 2469-9985, 2469-9993. DOI: 10.1103/PhysRevC.94.065801. URL: <https://link.aps.org/doi/10.1103/PhysRevC.94.065801>.
- [39] H. C. Mastwijk et al. “Optical Collisions of Cold, Metastable Helium Atoms”. In: *Phys. Rev. Lett.* 80 (25 June 1998), pp. 5516–5519. DOI: 10.1103/PhysRevLett.80.5516. URL: <https://link.aps.org/doi/10.1103/PhysRevLett.80.5516>.
- [40] J M McNamara et al. “Heteronuclear ionizing collisions between laser-cooled metastable helium atoms”. In: *Physical Review A* (75 2007), p. 062715. DOI: 10.1103/PhysRevA.75.062715.
- [41] Harold J. Metcalf and Peter van der Straten. *Laser Cooling and Trapping of Neutral Atoms*. Springer, 1999.
- [42] S. Moal et al. “Accurate Determination of the Scattering Length of Metastable Helium Atoms Using Dark Resonances between Atoms and Exotic Molecules”. In: *Phys. Rev. Lett.* 96.2 (Jan. 2006). DOI: 10.1103/physrevlett.96.023203. URL: <https://journals.aps.org/prl/abstract/10.1103/PhysRevLett.96.023203>.
- [43] C Orzel et al. “Spin polarization and quantum-statistical effects in ultracold ionizing collisions”. In: *Physical Review A* 59 (1999), pp. 1926–1935.
- [44] Spoden P et al. “Collisional Properties of Cold Spin-Polarized Metastable Neon Atoms”. In: *Physical Review Letters* 94 (2005).
- [45] Dany Page et al. “Rapid Cooling of the Neutron Star in Cassiopeia A Triggered by Neutron Superfluidity in Dense Matter”. In: *Phys. Rev. Lett.* (2011), p. 4. URL: <https://journals.aps.org/prl/abstract/10.1103/PhysRevLett.106.081101>.
- [46] G. B. Partridge et al. “Bose-Einstein condensation and spin mixtures of optically trapped metastable helium”. In: *Phys. Rev. A* 81 (5 May 2010), p. 053631. DOI: 10.1103/PhysRevA.81.053631. URL: <https://link.aps.org/doi/10.1103/PhysRevA.81.053631>.
- [47] Oliver Penrose and Lars Onsager. “Bose-Einstein Condensation and Liquid Helium”. In: *Phys. Rev.* 104 (3 Nov. 1956), pp. 576–584. DOI: 10.1103/PhysRev.104.576. URL: <https://link.aps.org/doi/10.1103/PhysRev.104.576>.
- [48] C Pethick and H Smith. *Bose-Einstein condensation in dilute gases*. Cambridge University Press, 2002.

- [49] L Pitaevskii and S Stringari. *Bose-Einstein Condensation*. Oxford University Publications, 2016.
- [50] N. R. Poniatowski. “Superconductivity, broken gauge symmetry, and the Higgs mechanism”. In: *American Journal of Physics* 87 (436 2019). DOI: 10.1119/1.5093291.
- [51] M Przybytek and B Jeziorski. “Bounds for the scattering length of spin-polarized helium from high-accuracy electronic structure calculations”. In: *Journal of Chemical Physics* (123 2005). DOI: <https://doi.org/10.1063/1.2042453>.
- [52] C C Bradley and C A Sackett, J J Tollett, and G Hulet. “evidence of Bose-Einstein condensation in an atomic gas with attractive interactions”. In: *physical review letters* 75 (1995), pp. 1687–1690. DOI: <https://doi.org/10.1103/PhysRevLett.75.1687>.
- [53] M. Schellekens et al. “Hanbury Brown Twiss effect for ultracold quantum gases”. In: *Science* 310 (2005). DOI: 10.1126/science.1118024.
- [54] Julian Schmitt et al. “Spontaneous Symmetry Breaking and Phase Coherence of a Photon Bose-Einstein Condensate Coupled to a Reservoir”. In: *Phys. Rev. Lett.* 116 (3 2016), p. 033604. DOI: 10.1103/PhysRevLett.116.033604. URL: <https://link.aps.org/doi/10.1103/PhysRevLett.116.033604>.
- [55] G. V. Shlyapnikov et al. “Decay Kinetics and Bose Condensation in a Gas of Spin-Polarized Triplet Helium”. In: *Phys. Rev. Lett.* 73 (24 Dec. 1994), pp. 3247–3250. DOI: 10.1103/PhysRevLett.73.3247. URL: <https://link.aps.org/doi/10.1103/PhysRevLett.73.3247>.
- [56] Robert P. Smith et al. “Effects of Interactions on the Critical Temperature of a Trapped Bose Gas”. In: *Phys. Rev. Lett.* 106 (25 June 2011), p. 250403. DOI: 10.1103/PhysRevLett.106.250403. URL: <https://link.aps.org/doi/10.1103/PhysRevLett.106.250403>.
- [57] R J W Stas et al. “Homonuclear ionizing collisions of laser-cooled metastable helium atoms”. In: *Physical Review A* (73 2006), p. 032713. DOI: 10.1103/PhysRevA.73.032713.
- [58] András Sütő. “Equivalence of Bose-Einstein Condensation and Symmetry Breaking”. In: *Phys. Rev. Lett.* 94 (8 Mar. 2005), p. 080402. DOI: 10.1103/PhysRevLett.94.080402. URL: <https://link.aps.org/doi/10.1103/PhysRevLett.94.080402>.
- [59] Naaman Tammuz et al. “Can a Bose Gas Be Saturated?” In: *Phys. Rev. Lett.* 106 (23 June 2011), p. 230401. DOI: 10.1103/PhysRevLett.106.230401. URL: <https://link.aps.org/doi/10.1103/PhysRevLett.106.230401>.
- [60] Paul J. J. Tol et al. “Large numbers of cold metastable helium atoms in a magneto-optical trap”. In: *Phys. Rev. A* 60 (2 Aug. 1999), R761–R764. DOI: 10.1103/PhysRevA.60.R761. URL: <https://link.aps.org/doi/10.1103/PhysRevA.60.R761>.
- [61] Andrey Tychkov. “Bose-Einstein Condensation of Metastable Helium Atoms”. PhD thesis. Vrije Universiteit Amsterdam, 2008.
- [62] W. Vassen et al. “Ultracold metastable helium: Ramsey fringes and atom interferometry”. In: *Applied Physics B* 122.12 (Nov. 2016). DOI: 10.1007/s00340-016-6563-0. URL: <https://link.springer.com/article/10.1007/s00340-016-6563-0>.
- [63] V. Venturi et al. “Close-coupled calculation of collisions of magnetostatically trapped metastable helium atoms”. In: *Phys. Rev. A* 60 (6 Dec. 1999), pp. 4635–4646. DOI: 10.1103/PhysRevA.60.4635. URL: <https://link.aps.org/doi/10.1103/PhysRevA.60.4635>.
- [64] John Weiner et al. “Experiments and theory in cold and ultracold collisions”. In: *Rev. Mod. Phys.* 71 (1 Jan. 1999), pp. 1–85. DOI: 10.1103/RevModPhys.71.1. URL: <https://link.aps.org/doi/10.1103/RevModPhys.71.1>.

- [65] V. I. Yukalov. “Basics of Bose-Einstein condensation”. In: *Physics of Particles and Nuclei* 42 (3 2011), pp. 460–513. DOI: 10.1134/S1063779611030063.
- [66] V. I. Yukalov. “Bose-Einstein condensation and gauge symmetry breaking”. In: *Laser physics letters* 4 (9 2007), pp. 632–647. DOI: 10.1002/lap1.200710029.